HHS Public Access

Author manuscript

Cortex. Author manuscript; available in PMC 2016 August 01.

Published in final edited form as:

Cortex. 2015 August ; 69: 121–130. doi:10.1016/j.cortex.2015.04.022.

Spatiotemporal oscillatory dynamics during the encoding and maintenance phases of a visual working memory task

Elizabeth Heinrichs-Graham[a,b] and **Tony W. Wilson**[b,c,d,CA]

[a]Department of Psychology, University of Nebraska – Omaha, Omaha, NE, USA

[b]Center for Magnetoencephalography, University of Nebraska Medical Center (UNMC), Omaha, NE, USA

[c]Department of Pharmacology and Experimental Neuroscience, UNMC, Omaha, NE, USA

[d]Department of Neurological Sciences, UNMC, Omaha, NE, USA

Abstract

Many electrophysiology studies have examined neural oscillatory activity during the encoding, maintenance, and/or retrieval phases of various working memory tasks. Together, these studies have helped illuminate the underlying neural dynamics, although much remains to be discovered and some findings have not replicated in subsequent work. In this study, we examined the oscillatory dynamics that serve visual working memory operations using high-density magnetoencephalography (MEG) and advanced time-frequency and beamforming methodology. Specifically, we recorded healthy adults while they performed a high-load, Sternberg-type working memory task, and focused on the encoding and maintenance phases. We found significant 9–16 Hz desynchronizations in the bilateral occipital cortices, left dorsolateral prefrontal cortex (DLPFC), and left superior temporal areas throughout the encoding phase. Our analysis of the dynamics showed that the left DLPFC and superior temporal desynchronization became stronger as a function of time during the encoding period, and was sustained throughout most of the maintenance phase until sharply decreasing in the milliseconds preceding retrieval. In contrast, desynchronization in occipital areas became weaker as a function of time during encoding and eventually evolved into a strong synchronization during the maintenance period, consistent with previous studies. These results provide clear evidence of dynamic network-level processes during the encoding and maintenance phases of working memory, and support the notion of a dynamic pattern of functionally-discrete subprocesses within each working memory phase. The presence of such dynamic oscillatory networks may be a potential source of inconsistent findings in this literature, as neural activity within these networks changes dramatically with time.

Corresponding Author: Tony W. Wilson, Ph.D., Center for Magnetoencephalography, University of Nebraska Medical Center, 988422 Nebraska Medical Center, Omaha, NE 68198, Phone: (402) 552-6431, Fax: (402) 559-5747, Tony.W.Wilson@gmail.com.

Keywords

magnetoencephalography; MEG; short-term memory; electrophysiology; network

1. Introduction

Working memory refers to the short-term storage and manipulation of information for immediate cognitive processing. Conceptually speaking, a stimulus can be loaded or "encoded" into working memory, stored and refreshed through some form of rehearsal or "maintenance" of the memory trace, and ultimately utilized or "retrieved" to perform a goal-oriented action; the information is then discarded or allowed to fully "decay." There are a number of different neurocognitive models of working memory (e.g, (Baddeley, 1992; Baddeley, 2000; Baddeley et al., 2011; D'Esposito, 2007), but all support the existence of encoding, maintenance, and retrieval phases as being necessary for successful working memory retention.

Many functional magnetic resonance imaging (fMRI) and positron-emission tomography (PET) investigations have examined working memory circuits in healthy adults (e.g., (Cabeza and Nyberg, 2000; Rottschy et al., 2012). These studies have highlighted a group of brain regions that include the dorsolateral prefrontal cortex, parietal and occipital regions, and the left supramarginal gyrus as critical to working memory function (Cabeza and Nyberg, 2000; Rottschy et al., 2012). While these PET and fMRI studies have provided valuable information on the specific brain regions that are active during working memory operations, delineating the brain areas that are active during each phase (i.e., encoding, maintenance, retrieval) of working memory processing has been more difficult due to the temporal limitations of these imaging modalities. However, recent neurophysiological investigations using magnetoencephalography (MEG) and electroencephalography (EEG), which possess excellent temporal resolution, have begun to fill this void by clarifying the spatiotemporal dynamics of working memory processing (e.g., (Bonnefond and Jensen, 2012; Bonnefond and Jensen, 2013; Brookes et al., 2011; Honkanen et al., 2014; Jensen et al., 2002; Jensen and Tesche, 2002; Jiang et al., 2015; Morgan et al., 2011; Palva et al., 2010a; Palva et al., 2011; Palva et al., 2010b; Roux and Uhlhaas, 2014; Roux et al., 2012; Sauseng et al., 2009; Spitzer et al., 2013)). While some findings in the MEG/EEG working memory literature have been variable, much of this variability can be attributed to task and stimulus design features (e.g., Sternberg versus N-back, auditory versus visual, verbal versus spatial). For example, neurophysiological studies of working memory have used auditory (Nolden et al., 2013; van Dijk et al., 2010), visuospatial (Jensen et al., 2002; Jensen et al., 2007; Jensen and Tesche, 2002; Palva et al., 2010a; Palva et al., 2011; Palva et al., 2010b), vibrotactile (Spitzer et al., 2013), and language-based stimuli (Brookes et al., 2011). Slight variations in task design were also the norm in fMRI and PET studies, and many of the inconsistencies in this literature are likely attributable to this factor (Cabeza and Nyberg, 2000; Rottschy et al., 2012).

Jensen and Tesche (2002) recorded MEG on healthy younger adults during a visual Sternberg task (Sternberg, 1969) and found that theta (4–7 Hz) activity in the frontal cortices parametrically increased as a function of memory load during the memory maintenance

phase, becoming stronger in amplitude from the 1-item condition up to the 7-item condition (Jensen and Tesche, 2002). Similar results have been reported by Gevins et al. (1997) and more recently by Sheeringa and colleagues (2009). Likewise, a MEG study by Brookes and colleagues (2011) also found an increase in frontal theta activity relative to the baseline, and a positive correlation between task difficulty and frontal theta. However, it is important to note that Brookes et al. did not distinguish between the encoding, maintenance, and retrieval phases so it is unclear which cognitive processes were best reflected in their images of oscillatory activity. In a related EEG study, Jensen et al. (2002) found that alpha (8–14 Hz) activity in the central parieto-occipital areas increased as a function of memory load during the maintenance phase, being weakest in the 2-item condition and strongest in the 6-item condition (Jensen et al., 2002). This pattern of increased alpha has been replicated and expanded in many recent studies, and findings of increased alpha during the maintenance phase appear to be especially robust (Bonnefond and Jensen, 2012; Bonnefond and Jensen, 2013; Jiang et al., 2015; Tuladhar et al., 2007). In contrast to these studies of working memory maintenance, Palva et al. (2011) reported that the amplitude of theta-alpha, high alpha, beta, and gamma activity were significantly reduced during the maintenance phase relative to the baseline phase in most brain areas, and in no regions was neuronal activity (at any frequency) significantly stronger during the maintenance phase relative to the baseline (Palva et al., 2011). Furthermore, they found that only high-alpha, beta, and gamma-frequency activity was positively correlated with memory load in the prefrontal cortices; that is, suppression of activity in these frequency bands became weaker as memory load increased (Palva et al., 2011). These and other discrepancies between studies may be attributable to not only focusing on different temporal phases of working memory (i.e., interpretations of what encompasses encoding, maintenance, or retrieval), but also focusing on distinct temporal periods within each phase across studies.

In the current study, we examined the dynamic distributed processes that serve working memory during a visual task that used single-letter stimuli that were simultaneously presented. Specifically, we focused on neural dynamics within the encoding and maintenance phases of working memory processing, where information is loaded, retained, and rehearsed. Prior EEG/MEG studies have not focused on the changing oscillatory dynamics within the encoding and maintenance periods specifically, which may lead to greater insight into the source of inconsistencies in this literature. To this end, we utilized high-density MEG to record healthy adult participants while they performed a modified, high-load, Sternberg-type working memory task. We hypothesized that participants would show relatively continuous neuronal activity across the encoding and maintenance periods in the left prefrontal and supramarginal regions, along with a dynamic response pattern in the occipital cortices, as function in this brain region switches from encoding stimuli to protecting active representations from incoming interference.

2. Methods

2.1 Subject Selection

We studied 16 healthy right-handed males (mean age: 26.00, range 19–30), all of whom were recruited from the local community. Exclusionary criteria included any medical illness

affecting CNS function, neurological or psychiatric disorder, history of head trauma, current substance abuse, and the MEG Laboratory's standard exclusion criteria (e.g., dental braces, metal implants, battery operated implants, and/or any type of ferromagnetic implanted material). After complete description of the study was given to participants, written informed consent was obtained following the guidelines of the University of Nebraska Medical Center's Institutional Review Board, which approved the study protocol.

2.2 Experimental Paradigm

During MEG recording, participants were seated in a nonmagnetic chair within the magnetically-shielded room and instructed to fixate on a crosshair presented centrally. A grid (19 × 13 cm; width by height) containing six letters was then presented and remained on-screen for 2 seconds. The letters then disappeared from the grid, and 3 seconds later a single "probe" letter appeared. Participants were instructed to tap their index finger if the probe letter was one of the six letters previously presented in the stimulus encoding set. Each trial lasted 6.9 s, including a 1.0 s pre-stimulus fixation; see Figure 1 for an illustration of the overall task design. Each participant completed 128 trials, and the task lasted approximately 14 minutes.

2.3 MEG data acquisition

All recordings were conducted in a one-layer magnetically-shielded room (MSR) with active shielding engaged. With an acquisition bandwidth of 0.1–330 Hz, neuromagnetic responses were sampled continuously at 1 kHz using an Elekta Neuromag system with 306 magnetic sensors (Elekta, Helsinki, Finland). Using MaxFilter (v2.1.15; Elekta), MEG data from each subject were individually corrected for head motion and subjected to noise reduction using the signal space separation method with a temporal extension (Taulu and Simola, 2006; Taulu et al., 2005). For motion correction, the position of the head throughout the recording was aligned to the individual's head position when the recording was initiated.

2.4 MEG Coregistration & Structural MRI Processing

Prior to MEG measurement, four coils were attached to the subject's head and localized, together with the three fiducial points and scalp surface, with a 3-D digitizer (Fastrak 3SF0002, Polhemus Navigator Sciences, Colchester, VT, USA). Once the subject was positioned for MEG recording, an electric current with a unique frequency label (e.g., 322 Hz) was fed to each of the coils. This induced a measurable magnetic field and allowed each coil to be localized in reference to the sensors throughout the recording session. Since coil locations were also known in head coordinates, all MEG measurements could be transformed into a common coordinate system. With this coordinate system, each participant's MEG data were coregistered with structural T1-weighted MRI data prior to source space analyses using BESA MRI (Version 2.0). Structural MRI data were aligned parallel to the anterior and posterior commissures and transformed into the Talairach coordinate system (Talairach and Tournoux, 1988). Following source analysis (i.e., beamforming), each subject's functional images were transformed into standardized space using the transform applied to the structural MRI volume.

2.5 MEG Time-Frequency Transformation and Statistics

Cardio and eyeblink artifacts were removed from the data using signal-space projection (SSP), which was accounted for during source reconstruction (Uusitalo and Ilmoniemi, 1997). The continuous magnetic time series was divided into epochs of 6.9 s duration, with baseline being defined as −0.4 to 0.0 s before initial stimulus onset (see Figure 1). Epochs containing artifacts were rejected based on a fixed threshold method, supplemented with visual inspection. An average of 91.69 (SD: 8.28) trials were used for further analysis.

Artifact-free epochs were transformed into the time-frequency domain using complex demodulation (resolution: 2.0 Hz, 25 ms; (Papp and Ktonas, 1977)), and the resulting spectral power estimations per sensor were averaged over trials to generate time-frequency plots of mean spectral density. These sensor-level data were normalized by dividing the power value of each time-frequency bin by the respective bin's baseline power, which was calculated as the mean power during the −0.4 to 0 s time period. This normalization allowed task-related power fluctuations to be visualized in sensor space. However, since there is considerable variability in the time-frequency windows examined across different neurophysiological studies of working memory, the time-frequency windows subjected to beamforming (i.e., imaging) in this study were derived through a purely data-driven approach.

The specific time-frequency windows used for imaging were determined by statistical analysis of the sensor-level spectrograms across the entire array of gradiometers (magnetometer data was not analyzed) during the five-second "encoding" and "maintenance" time windows; see Figure 1. We focused on the gradiometer data because these sensors have a higher SNR for cortical activity, which is what was primarily expected given the known cortical origins of working memory. Each data point in the spectrogram was initially evaluated using a mass univariate approach based on the general linear model. To reduce the risk of false positive results while maintaining reasonable sensitivity, a two stage procedure was followed to control for Type 1 error. In the first stage, one-sample t-tests were conducted on each data point and the output spectrogram of t-values was thresholded at $p < 0.05$ to define time-frequency bins containing potentially significant oscillatory deviations across all participants. In stage two, time-frequency bins that survived the threshold were clustered with temporally and/or spectrally neighboring bins that were also above the ($p < 0.05$) threshold, and a cluster value was derived by summing all of the t-values of all data points in the cluster. Nonparametric permutation testing was then used to derive a distribution of cluster-values and the significance level of the observed clusters (from stage one) were tested directly using this distribution (Ernst, 2004; Maris and Oostenveld, 2007). For each comparison, at least 10,000 permutations were computed to build a distribution of cluster values. Based on these analyses, the time-frequency windows that contained significant oscillatory events across all participants during the encoding and maintenance phases were subjected to the beamforming analysis.

2.6 MEG Source Imaging & Statistics

Cortical networks were imaged through an extension of the linearly constrained minimum variance vector beamformer (Hillebrand et al., 2005; Liljestrom et al., 2005; Van Veen et

al., 1997), which employs spatial filters in the frequency domain to calculate source power for the entire brain volume. The single images are derived from the cross spectral densities of all combinations of MEG gradiometers averaged over the time-frequency range of interest, and the solution of the forward problem for each location on a grid specified by input voxel space. Following convention, we computed noise-normalized, differential source power per voxel in each participant using active (i.e., task) and passive (i.e., baseline) periods of equal duration and bandwidth (Hillebrand et al., 2005). Such images are typically referred to as pseudo-t maps, with units (i.e., pseudo-t) that reflect noise-normalized power differences per voxel. MEG preprocessing and imaging used the Brain Electrical Source Analysis (BESA version 6.0) software.

Normalized differential source power was computed for the selected time-frequency bands, using a common baseline, over the entire brain volume per participant at 4.0 × 4.0 × 4.0 mm resolution. The effect of time was examined using a random effects analysis for the time-frequency bins of interest. Paired-sample t-tests were conducted to probe temporal changes in activation patterns between each of the 0.4 s time bins examined during the encoding and maintenance phases. As with the sensor-level analysis, a two-stage approach was used to control for Type 1 error, while maintaining reasonable sensitivity. In the first stage, one-sample or paired t-tests were conducted on the pseudo-t values of each voxel and the output was thresholded at ($p < 0.05$) to create statistical parametric maps (SPMs) showing clusters of potentially significant responses (one-sample) or temporal differences in response amplitude (paired-samples). A cluster t-value was derived in stage two, for each cluster surviving stage one, by summing all of the t-values of all data points (voxels) within the cluster. Subsequently, we used permutation testing to derive a distribution of cluster t-values, and tested the observed clusters for statistical significance using this distribution (Ernst, 2004; Maris and Oostenveld, 2007). For each comparison, at least 1,000 permutations were computed to build a distribution of cluster t-values.

3. Results

All 16 participants were able to successfully complete the task. Participants performed generally well, correctly identifying the probe in 84.18% (SD: 6.74%) of all trials. Specifically, participants had a correct hit rate of 0.719, and a false alarm rate of 0.036, $d' = 2.377$. Only correct trials were used for analysis.

3.1 Sensor-Level Analysis

Analysis of the encoding and maintenance time windows showed a significant cluster of decreased high alpha/low beta (9–16 Hz) oscillatory power that began 0.2 s after onset of the stimulus grid and was sustained throughout the duration of the encoding phase and slightly into the maintenance phase (Figure 2), in the frontal and posterior gradiometers ($p < .001$, corrected). To probe how these oscillations evolved as a function of time, this significant time window was split into four non-overlapping 0.4 s time bins for the encoding phase (0.2 – 1.8 s) and a transition period from encoding to maintenance (1.8 – 2.2 s); these time-frequency bins were imaged using beamforming. In addition, a significant cluster of increased 9–12 Hz alpha activity was detected during the majority of the maintenance phase ($p < .001$, corrected), and this time window was split into eight non-overlapping time bins of

0.4 s each (1.8 – 5.0 s) and subjected to a beamformer analysis to evaluate the temporal dynamics of working memory processing.

3.2 Beamformer Analysis

The specific 9–16 Hz time bins subjected to beamforming were as follows: Encoding 1: 0.2 – 0.6 s; Encoding 2: 0.6 – 1.0 s; Encoding 3: 1.0 – 1.4 s; Encoding 4: 1.4 – 1.8 s; Transition: 1.8 – 2.2 s. Sequential beamformer output images from these time periods were computed using a common baseline period (−0.4 to 0.0 s), and the resulting pseudo-t units were compared using paired-samples t-tests, with each comparison being subjected to permutation testing. The onset of the encoding grid at 0.0 s initiated a strong 9–16 Hz decrease in occipital and other posterior cortices (Figure 2), which gradually spread anteriorly into left temporal and frontal cortices. From Encoding 1 to Encoding 2, the 9–16 Hz activity increased in the right superior temporal sulcus ($p < .001$, corrected), while activity in the left DLPFC and supramarginal gyrus further decreased (both *p's* < .001, corrected; Figure 3). From Encoding 2 to Encoding 3, 9–16 Hz activity in bilateral occipital cortices started to increase towards baseline levels ($p < .001$, corrected), while activity in the left DLPFC continued to decrease, and significant decreases also emerged in the left superior temporal gyrus ($p < 0.001$, corrected). Finally, from Encoding 3 to Encoding 4 there continued to be a significant increase in alpha/beta power in bilateral occipital cortices ($p < .001$, corrected; Figure 3), which continued from Encoding 4 to the transition period between encoding and maintenance ($p < .001$, corrected). Beyond these dynamics, there was a strong and sustained decrease in alpha/beta activity throughout most of the encoding phase in the left middle and superior temporal gyri, left supramarginal gyrus, and the left inferior frontal gyrus ($p < 0.000001$; one-sample t-test per time window). A map of group-mean responses per time window is shown in Figure 4.

As with the encoding period, sequential beamformer output images from the maintenance phase time periods were computed using a common baseline (−0.4 to 0.0 s) and compared using paired-samples t-tests, with each comparison being subjected to permutation testing. The specific 9–12 Hz time bins subjected to beamforming were: Transition: 1.8 – 2.2 s; Maintenance 1: 2.2 – 2.6 s; Maintenance 2: 2.6 – 3.0 s; Maintenance 3: 3.0 – 3.4 s; Maintenance 4: 3.4 – 3.8 s; Maintenance 5: 3.8 – 4.2 s; Maintenance 6: 4.2 – 4.6 s; Maintenance 7: 4.6 – 5.0 s (probe onset = 5.0 s). From the Transition to the Maintenance 1 period, alpha activity in the parietal-occipital sulcus region continued to increase towards baseline levels with time (i.e., similar to the encoding phase). Similar effects were seen in the right cerebellum, where alpha activity increased from Transition to Maintenance 1 (both *p's* < 0.001, corrected). These increases in alpha within the cerebellum and occipital continued from Maintenance 1 to Maintenance 2 ($p < 0.001$, corrected), and from Maintenance 2 to Maintenance 3 ($p < 0.001$, corrected), where both responses significantly rebounded above baseline levels. This oscillatory shift is shown in Figure 5. Significant oscillatory changes continued in the cerebellum from Maintenance 3 to Maintenance 4 and 5. From Maintenance 5 to 6, 9–12 Hz activity in occipital and right cerebellar cortices significantly decreased, and this decrease continued from Maintenance period 6 to 7 in these brain regions (both *p's* < .001, corrected). In contrast, activity in the left superior temporal gyrus and left inferior frontal gyrus significantly increased towards baseline levels from the

Maintenance 6 to the Maintenance 7 time period ($p < .001$, corrected). Finally, as with the encoding phase, alpha activity in the left middle and superior temporal gyri, supramarginal gyrus, and left inferior frontal gyrus was sustained throughout the maintenance phase ($p < 0.000001$; one-sample t-test per time bin), although activity clearly increased toward baseline levels near the end of the maintenance aspect of the task.

4. Discussion

In the current study, we investigated the oscillatory dynamics that serve working memory encoding and maintenance in healthy adults who were performing a Sternberg-type working memory task. Most importantly, we found that presentation of the encoding grid elicited a strong decrease in 9–16 Hz activity in the occipital cortices that was sustained for about 1.0 s, and then gradually returned to baseline throughout the encoding and the beginning of the maintenance period (9–12 Hz), before strongly increasing during the final second before retrieval. In contrast, high alpha/low beta activity in the left temporal and prefrontal areas significantly decreased as a function of time during the encoding period, and such activity was sustained throughout most of the maintenance phase until sharply increasing toward baseline levels during the final second leading up to retrieval. Together, these results indicate that working memory functions are supported by widespread temporal dynamics and enhance understanding of the complex neurophysiological processes that serve working memory encoding and maintenance in healthy adults.

We found strong decreases in alpha/beta (9–16 Hz) activity in the bilateral occipital cortices shortly after onset of the encoding grid. Given the visual nature of our stimuli (i.e., letters embedded in a grid), this was not surprising as alpha decreases following visual stimulation were reported in the earliest MEG paper (Cohen, 1968) and have been widely described since then. In regard to the duration of the response, Ihara and Kakigi (2006) found strong, sustained alpha decreases in the bilateral occipital areas of bilingual speakers during a visual perception task, which were strongest during the visual processing of letters from the participants' first language. Such a prolonged response is certainly in agreement with our findings, as a strong decrease in occipital alpha/beta was readily apparent until early in the maintenance phase of the task (i.e., 2.6 s after grid onset). Recent neurophysiological evidence also suggests that this early decrease in the occipital cortices is modulated by visuospatial attention (Gould et al., 2011).

Beginning about 1.0 s after the onset of the maintenance period, significant alpha activity transitioned from a strong decrease to a robust increase in the parieto-occipital sulcus area. Alpha increases (i.e., synchronization) in the parieto-occipital sulcus have been reliably correlated with both memory load and, more importantly, the successful inhibition of distracters during working memory maintenance (Bonnefond and Jensen, 2012; Jensen et al., 2002; Tuladhar et al., 2007). For example, Bonnefond and Jensen (2012) used alphabetic stimuli and introduced either a weak distractor (a symbol) or a strong distractor (another letter) during the maintenance phase of a working memory task. They found that parieto-occipital alpha increased in anticipation of the distractor, and that the amplitude of parieto-occipital alpha was higher during the maintenance phase when a strong distracter was present (2012). While we did not specifically manipulate distracters, we did track the time

course of occipital alpha and found that the amplitude of activity was more prominent in the later stages of working memory, when the likelihood of forgetting should be increasing. These findings support the hypothesis that alpha increases (synchronization) in the occipital cortices reflect inhibition of sensory cortices to "gate" incoming stimuli. Interestingly, we further found that this occipital increase started to dissipate in the final time bin preceding retrieval, which may suggest that inhibition decreases as retrieval processes are initiated. We found a similar pattern of responses in the cerebellar cortices (especially right cerebellum). A large amount of work has been done to investigate the role of the cerebellum in working memory (see (Marvel and Desmond, 2010), and the general consensus is that cerebellar lobe VIII is preferentially activated when information is maintained for retrieval, which is consistent with our findings (Marvel and Desmond, 2010). We acknowledge that there is still some debate about the sensitivity of MEG to cerebellar activity. However, in our view, good practice is to present the data as observed and let the findings be confirmed (or not) by future work. We should point out that the number of MEG papers reporting cerebellar activity is growing (Bourguignon et al., 2013; Bourguignon et al., 2012; Dalal et al., 2008; Dalal et al., 2007; Krause et al., 2010; Maratos et al., 2007; Pollok et al., 2008; Pollok et al., 2009; Soto and Jerbi, 2012; Timmermann et al., 2003; Wilson et al., 2010; Wilson et al., 2011; Wilson et al., 2009).

Beyond the occipital and cerebellar cortices, we observed sustained alpha/beta decreases in the left DLPFC, left middle temporal, and left supramarginal areas, which progressively decreased during encoding, and maintained the same amplitude throughout most of the maintenance phase until returning to baseline just before retrieval. All of these left hemispheric brain regions are known to be involved in language processing and have been previously implicated in working memory studies, especially those that propose a multicomponent model of working memory like that of Baddeley and colleagues (Baddeley, 1992; Baddeley, 2000; Baddeley et al., 2011; Baddeley and Hitch, 1974; Baddeley, 1974). In Baddeley's framework, there are two slave systems that function to maintain short term information, a central executive mechanism that is responsible for deciding what information is relevant and which pieces of information can be integrated, and an episodic buffer component that is responsible for integrating data from the two slave systems (for extensive reviews, see (Baddeley, 2000; Baddeley et al., 2011). Studies have linked the left DLPFC and inferior frontal gyrus to executive functioning (i.e., the central executive component) and these two areas were engaged during encoding and remained active throughout the maintenance phase in our study. Further, the first slave system, the phonological loop, stores language-based information and keeps these data current through forms of rehearsal, which likely involves frontal areas. Previous meta-analytic fMRI studies have connected the left superior temporal lobe and left supramarginal gyrus to engagement of the so-called phonological loop (Cabeza and Nyberg, 2000; Rottschy et al., 2012) and our findings would be consistent with this position. Essentially, neural activity in the phonological loop should begin in the encoding phase and be sustained throughout the maintenance phase in language-based working memory tasks, which is in agreement with the dynamics we observed in the left superior temporal and supramarginal areas. Presumably, the extensive co-activation of frontal and temporal regions reflects interactions needed to store (superior temporal and supramarginal) and guide rehearsal of information

(DLPFC) until retrieval processes are initiated. Far less is known about the neurological correlates of the episodic buffer and we can only speculate that such processing may involve tissues in the left temporal lobe, as a large area of this brain region was engaged through most of the encoding and maintenance phases of our task. Lastly, the other slave system, the visuo-spatial sketch pad, stores visual and spatial information. Our task did not involve a spatial memory component and thus likely did not require this component.

The left DLPFC has also been shown to selectively respond to the identification and storage of word and letter information used in working memory (Chan, 2013; Liu et al., 2009), and this area is widely known as an executive hub for cognitive and attentional control (e.g., (Fried et al., 2014; Goldman-Rakic et al., 1992). Chen and Lin (2012) used MEG to record participants while they processed abstract and concrete words, and then tested participants on which words they later remembered. They found that, not only was the left DLPFC preferentially active during word processing, but that broadband activations were of higher amplitude when the words were later remembered (2012). Importantly, they found a slight delay in DLPFC activity, and suggested that this could be due to encoding inefficiency (Chen and Lin, 2012). While we arguably observed a similar “delay” (i.e., a temporal difference) in left DLPFC activity, this delay was due to a continuous decrease in 9–16 Hz activity throughout the encoding period, coupled with an increase in such activity in the bilateral occipital cortices. We suggest that this “delay” is not due to inefficiency, but rather is a function of the dynamic process by which the stimuli are being encoded from lower-level stimulus processing to higher-level executive and associative processing, which aids in later retrieval. Furthermore, we speculate that finer decomposition of the time series may indicate oscillatory dynamics in the millisecond range between the left DLPFC and supramarginal area, reflecting active rehearsal mechanisms to maintain the memory trace. In future studies, we plan to focus on the maintenance phase of working memory and interrogate the dynamics on a finer scale (e.g., time bins of 10’s of milliseconds).

While this study provides critical insight into the spatiotemporal dynamics of the encoding and maintenance phases of working memory processing, it is important to note some limitations. The primary results of this study highlight the importance of temporal information in understanding complex brain processes, such as that of encoding, rehearsing, and maintaining information during a working memory task. However, finer scale spectro-temporal analyses, as well as dynamic connectivity analyses, are needed to further determine how these different responses evolve on a millisecond level. Furthermore, it is likely that the strength of interregional interactions (i.e., functional connectivity) among active brain regions changes with each phase of the task, and thus connectivity indices will need to be computed on individual time bins in future studies. One potential limitation of this study is that we did not image theta frequency activity. Activity in the theta band was not significant in our permutation testing on sensor-level time-frequency data, and thus we did not attempt to resolve this activity using a beamformer. Typically, studies reporting frontal theta (e.g., (Brookes et al., 2011; Jensen and Tesche, 2002) presented stimuli sequentially during the encoding phase, and this may explain why significant theta was not observed in our experiment which used simultaneous presentation. Another limitation of our study is that the complexity of the task (e.g., memory load) was not parametrically varied. As such, interpretations of how these neuronal oscillations might differ as a function of memory load

can only be speculative in nature. Despite these limitations, the current study provides essential information regarding the pattern of neural activity that serves successful preservation of information in verbal working memory.

Acknowledgments

This work was supported by NIH grant R01 MH103220 (TWW), a Kinman-Oldfield Award for Neurodegenerative Research from the University of Nebraska Medical Center (TWW), and a grant from the Nebraska Banker's Association. The Center for Magnetoencephalography at the University of Nebraska Medical Center was founded through an endowment from an anonymous donor. The funders had no role in study design, data collection and analysis, decision to publish, or preparation of the manuscript.

References

Baddeley A. Working memory. Science. 1992; 255(5044):556–9. [PubMed: 1736359]

Baddeley A. The episodic buffer: a new component of working memory? Trends Cogn Sci. 2000; 4(11):417–423. [PubMed: 11058819]

Baddeley AD, Allen RJ, Hitch GJ. Binding in visual working memory: the role of the episodic buffer. Neuropsychologia. 2011; 49(6):1393–400. [PubMed: 21256143]

Baddeley, AD.; Hitch, GJ. Working Memory. In: Bower, GA., editor. The Psychology of Learning and Motivation: Advances in Research and Theory. New York: Academic Press; 1974. p. 47-89.

Baddeley, ADH.; GJ. Working Memory. In: Bower, GA., editor. The Psychology of Learning and Motivation: Advances in Research and Theory. New York: Academic Press; 1974. p. 47-89.

Bonnefond M, Jensen O. Alpha oscillations serve to protect working memory maintenance against anticipated distracters. Curr Biol. 2012; 22(20):1969–74. [PubMed: 23041197]

Bonnefond M, Jensen O. The role of gamma and alpha oscillations for blocking out distraction. Commun Integr Biol. 2013; 6(1):e22702. [PubMed: 23802042]

Bourguignon M, De Tiege X, de Beeck MO, Van Bogaert P, Goldman S, Jousmaki V, Hari R. Primary motor cortex and cerebellum are coupled with the kinematics of observed hand movements. Neuroimage. 2013; 66:500–7. [PubMed: 23108269]

Bourguignon M, Jousmaki V, Op de Beeck M, Van Bogaert P, Goldman S, De Tiege X. Neuronal network coherent with hand kinematics during fast repetitive hand movements. Neuroimage. 2012; 59(2):1684–91. [PubMed: 21963911]

Brookes MJ, Wood JR, Stevenson CM, Zumer JM, White TP, Liddle PF, Morris PG. Changes in brain network activity during working memory tasks: a magnetoencephalography study. Neuroimage. 2011; 55(4):1804–15. [PubMed: 21044687]

Cabeza R, Nyberg L. Imaging cognition II: An empirical review of 275 PET and fMRI studies. J Cogn Neurosci. 2000; 12(1):1–47. [PubMed: 10769304]

Chan AW. Functional organization and visual representations of human ventral lateral prefrontal cortex. Front Psychol. 2013; 4:371. [PubMed: 23847558]

Chen TC, Lin YY. High neuromagnetic activation in the left prefrontal and frontal cortices correlates with better memory performance for abstract words. Brain Lang. 2012; 123(1):42–51. [PubMed: 22902031]

Cohen D. Magnetoencephalography: evidence of magnetic fields produced by alpha-rhythm currents. Science. 1968; 161(3843):784–6. [PubMed: 5663803]

D'Esposito M. From cognitive to neural models of working memory. Philos Trans R Soc Lond B Biol Sci. 2007; 362(1481):761–72. [PubMed: 17400538]

Dalal SS, Guggisberg AG, Edwards E, Sekihara K, Findlay AM, Canolty RT, Berger MS, Knight RT, Barbaro NM, Kirsch HE, et al. Five-dimensional neuroimaging: localization of the time-frequency dynamics of cortical activity. Neuroimage. 2008; 40(4):1686–700. [PubMed: 18356081]

Dalal SS, Guggisberg AG, Edwards E, Sekihara K, Findlay AM, Canolty RT, Knight RT, Barbaro NM, Kirsch HE, Nagarajan SS. Spatial localization of cortical time-frequency dynamics. Conf Proc IEEE Eng Med Biol Soc. 2007; 2007:4941–4. [PubMed: 18003115]

Ernst MD. Permutation methods: A basis for exact inference. Stat Sci. 2004; 19:676–685.

Fried PJ, Rushmore RJ 3rd, Moss MB, Valero-Cabre A, Pascual-Leone A. Causal evidence supporting functional dissociation of verbal and spatial working memory in the human dorsolateral prefrontal cortex. Eur J Neurosci. 2014; 39(11):1973–81. [PubMed: 24713032]

Gevins A, Smith ME, McEvoy L, Yu D. High-resolution EEG mapping of cortical activation related to working memory: effects of task difficulty, type of processing, and practice. Cereb Cortex. 1997; 7(4):374–85. [PubMed: 9177767]

Goldman-Rakic PS, Bates JF, Chafee MV. The prefrontal cortex and internally generated motor acts. Curr Opin Neurobiol. 1992; 2(6):830–5. [PubMed: 1477547]

Gould IC, Rushworth MF, Nobre AC. Indexing the graded allocation of visuospatial attention using anticipatory alpha oscillations. J Neurophysiol. 2011; 105(3):1318–26. [PubMed: 21228304]

Hillebrand A, Singh KD, Holliday IE, Furlong PL, Barnes GR. A new approach to neuroimaging with magnetoencephalography. Hum Brain Mapp. 2005; 25(2):199–211. [PubMed: 15846771]

Honkanen R, Rouhinen S, Wang SH, Palva JM, Palva S. Gamma Oscillations Underlie the Maintenance of Feature-Specific Information and the Contents of Visual Working Memory. Cereb Cortex. 2014

Ihara A, Kakigi R. Oscillatory activity in the occipitotemporal area related to the visual perception of letters of a first/second language and pseudoletters. Neuroimage. 2006; 29(3):789–96. [PubMed: 16209929]

Jensen O, Gelfand J, Kounios J, Lisman JE. Oscillations in the alpha band (9–12 Hz) increase with memory load during retention in a short-term memory task. Cereb Cortex. 2002; 12(8):877–82. [PubMed: 12122036]

Jensen O, Kaiser J, Lachaux JP. Human gamma-frequency oscillations associated with attention and memory. Trends Neurosci. 2007; 30(7):317–24. [PubMed: 17499860]

Jensen O, Tesche CD. Frontal theta activity in humans increases with memory load in a working memory task. Eur J Neurosci. 2002; 15(8):1395–9. [PubMed: 11994134]

Jiang H, van Gerven MA, Jensen O. Modality-specific Alpha Modulations Facilitate Long-term Memory Encoding in the Presence of Distracters. J Cogn Neurosci. 2015; 27(3):583–92. [PubMed: 25244116]

Krause V, Schnitzler A, Pollok B. Functional network interactions during sensorimotor synchronization in musicians and non-musicians. Neuroimage. 2010; 52(1):245–51. [PubMed: 20363337]

Liljestrom M, Kujala J, Jensen O, Salmelin R. Neuromagnetic localization of rhythmic activity in the human brain: a comparison of three methods. Neuroimage. 2005; 25(3):734–45. [PubMed: 15808975]

Liu L, Deng X, Peng D, Cao F, Ding G, Jin Z, Zeng Y, Li K, Zhu L, Fan N, et al. Modality- and task-specific brain regions involved in Chinese lexical processing. J Cogn Neurosci. 2009; 21(8):1473–87. [PubMed: 18823229]

Maratos FA, Anderson SJ, Hillebrand A, Singh KD, Barnes GR. The spatial distribution and temporal dynamics of brain regions activated during the perception of object and non-object patterns. Neuroimage. 2007; 34(1):371–83. [PubMed: 17055298]

Maris E, Oostenveld R. Nonparametric statistical testing of EEG- and MEG-data. J Neurosci Methods. 2007; 164(1):177–90. [PubMed: 17517438]

Marvel CL, Desmond JE. The contributions of cerebro-cerebellar circuitry to executive verbal working memory. Cortex. 2010; 46(7):880–95. [PubMed: 19811779]

Morgan HM, Muthukumaraswamy SD, Hibbs CS, Shapiro KL, Bracewell RM, Singh KD, Linden DE. Feature integration in visual working memory: parietal gamma activity is related to cognitive coordination. J Neurophysiol. 2011; 106(6):3185–94. [PubMed: 21940605]

Nolden S, Grimault S, Guimond S, Lefebvre C, Bermudez P, Jolicoeur P. The retention of simultaneous tones in auditory short-term memory: A magnetoencephalography study. Neuroimage. 2013; 82C:384–392. [PubMed: 23751862]

Palva JM, Monto S, Kulashekhar S, Palva S. Neuronal synchrony reveals working memory networks and predicts individual memory capacity. Proc Natl Acad Sci U S A. 2010a; 107(16):7580–5. [PubMed: 20368447]

Palva S, Kulashekhar S, Hamalainen M, Palva JM. Localization of cortical phase and amplitude dynamics during visual working memory encoding and retention. J Neurosci. 2011; 31(13):5013–25. [PubMed: 21451039]

Palva S, Monto S, Palva JM. Graph properties of synchronized cortical networks during visual working memory maintenance. Neuroimage. 2010b; 49(4):3257–68. [PubMed: 19932756]

Papp N, Ktonas P. Critical evaluation of complex demodulation techniques for the quantification of bioelectrical activity. Biomed Sci Instrum. 1977; 13:135–45. [PubMed: 871500]

Pollok B, Gross J, Kamp D, Schnitzler A. Evidence for anticipatory motor control within a cerebello-diencephalic-parietal network. J Cogn Neurosci. 2008; 20(5):828–40. [PubMed: 18201129]

Pollok B, Krause V, Butz M, Schnitzler A. Modality specific functional interaction in sensorimotor synchronization. Hum Brain Mapp. 2009; 30(6):1783–90. [PubMed: 19301250]

Rottschy C, Langner R, Dogan I, Reetz K, Laird AR, Schulz JB, Fox PT, Eickhoff SB. Modelling neural correlates of working memory: a coordinate-based meta-analysis. Neuroimage. 2012; 60(1): 830–46. [PubMed: 22178808]

Roux F, Uhlhaas PJ. Working memory and neural oscillations: alpha-gamma versus theta-gamma codes for distinct WM information? Trends Cogn Sci. 2014; 18(1):16–25. [PubMed: 24268290]

Roux F, Wibral M, Mohr HM, Singer W, Uhlhaas PJ. Gamma-band activity in human prefrontal cortex codes for the number of relevant items maintained in working memory. J Neurosci. 2012; 32(36):12411–20. [PubMed: 22956832]

Sauseng P, Klimesch W, Heise KF, Gruber WR, Holz E, Karim AA, Glennon M, Gerloff C, Birbaumer N, Hummel FC. Brain oscillatory substrates of visual short-term memory capacity. Curr Biol. 2009; 19(21):1846–52. [PubMed: 19913428]

Scheeringa R, Petersson KM, Oostenveld R, Norris DG, Hagoort P, Bastiaansen MC. Trial-by-trial coupling between EEG and BOLD identifies networks related to alpha and theta EEG power increases during working memory maintenance. Neuroimage. 2009; 44(3):1224–38. [PubMed: 18840533]

Soto JL, Jerbi K. Investigation of cross-frequency phase-amplitude coupling in visuomotor networks using magnetoencephalography. Conf Proc IEEE Eng Med Biol Soc. 2012; 2012:1550–3. [PubMed: 23366199]

Spitzer B, Gloel M, Schmidt TT, Blankenburg F. Working Memory Coding of Analog Stimulus Properties in the Human Prefrontal Cortex. Cereb Cortex. 2013

Sternberg S. Memory-scanning: mental processes revealed by reaction-time experiments. Am Sci. 1969; 57(4):421–57. [PubMed: 5360276]

Talairach, G.; Tournoux, P. Co-planar stereotaxic atlas of the human brain. New York, NY: Thieme; 1988.

Taulu S, Simola J. Spatiotemporal signal space separation method for rejecting nearby interference in MEG measurements. Phys Med Biol. 2006; 51(7):1759–68. [PubMed: 16552102]

Taulu S, Simola J, Kajola M. Applications of the signal space separation method (SSS). IEEE Trans Signal Process. 2005; 53(9):3359–3372.

Timmermann L, Gross J, Dirks M, Volkmann J, Freund HJ, Schnitzler A. The cerebral oscillatory network of parkinsonian resting tremor. Brain. 2003; 126(Pt 1):199–212. [PubMed: 12477707]

Tuladhar AM, ter Huurne N, Schoffelen JM, Maris E, Oostenveld R, Jensen O. Parieto-occipital sources account for the increase in alpha activity with working memory load. Hum Brain Mapp. 2007; 28(8):785–92. [PubMed: 17266103]

Uusitalo MA, Ilmoniemi RJ. Signal-space projection method for separating MEG or EEG into components. Med Biol Eng Comput. 1997; 35(2):135–40. [PubMed: 9136207]

van Dijk H, Nieuwenhuis IL, Jensen O. Left temporal alpha band activity increases during working memory retention of pitches. Eur J Neurosci. 2010; 31(9):1701–7. [PubMed: 20525083]

Van Veen BD, van Drongelen W, Yuchtman M, Suzuki A. Localization of brain electrical activity via linearly constrained minimum variance spatial filtering. IEEE Trans Biomed Eng. 1997; 44(9): 867–80. [PubMed: 9282479]

Wilson TW, Slason E, Asherin R, Kronberg E, Reite ML, Teale PD, Rojas DC. An extended motor network generates beta and gamma oscillatory perturbations during development. Brain Cogn. 2010; 73(2):75–84. [PubMed: 20418003]

Wilson TW, Slason E, Asherin R, Kronberg E, Teale PD, Reite ML, Rojas DC. Abnormal gamma and beta MEG activity during finger movements in early-onset psychosis. Dev Neuropsychol. 2011; 36(5):596–613. [PubMed: 21667363]

Wilson TW, Slason E, Hernandez OO, Asherin R, Reite ML, Teale PD, Rojas DC. Aberrant high-frequency desynchronization of cerebellar cortices in early-onset psychosis. Psychiatry Res. 2009; 174(1):47–56. [PubMed: 19783411]

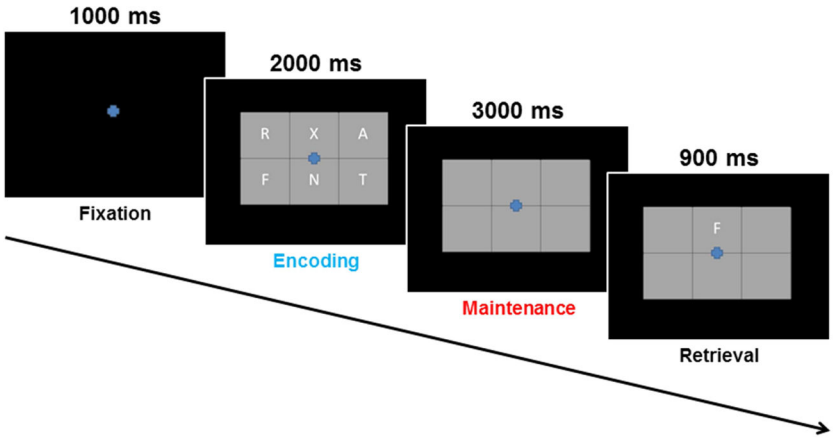

Figure 1.

Sternberg-Type Working Memory Paradigm. Each trial consisted of four phases: (1) a fixation phase which lasted 1.0 s and functioned as the baseline (−0.4 to 0 s), (2) an encoding phase (blue text) which lasted 2.0 s and consisted of 6 letters being presented simultaneously within a grid, (3) a maintenance phase (red text) lasting 3.0 s where the six letters disappeared from the grid, and (4) a retrieval phase which lasted 0.9 s and required participants to respond as to whether the single letter probe was included in the original encoding set.

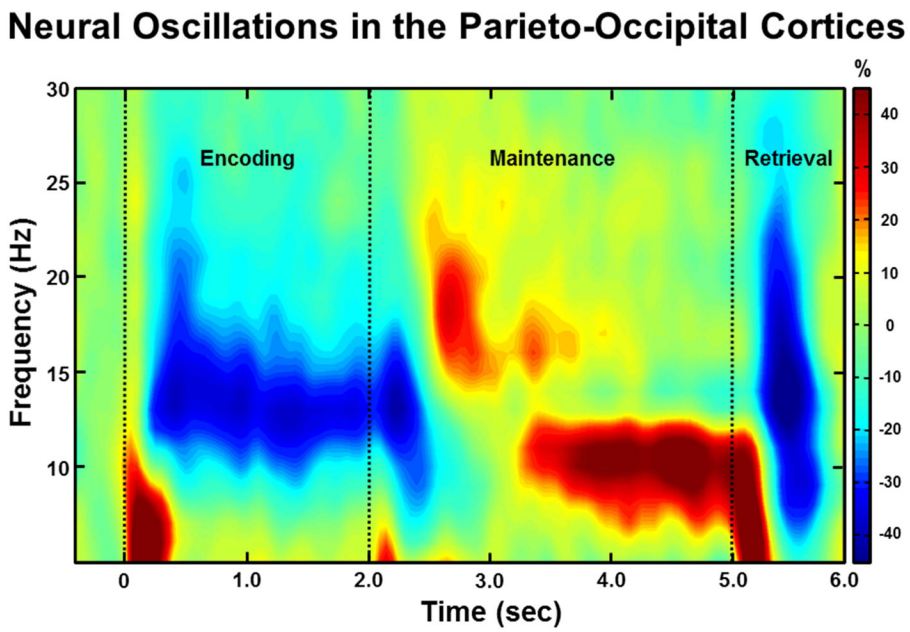

Figure 2.

Group-Averaged Time-Frequency Spectra During Encoding, Maintenance, and Retrieval Phases. Time (in ms) is denoted on the x-axis, with 0 ms defined as onset of the encoding grid. Frequency (in Hz) is shown on the y-axis. All signal power data is expressed as a percent difference from baseline (−0.4 to 0.0 s), with the color legend shown to the far right. Data represent a group-averaged gradiometer sensor that was near the parietal-occipital region in each participant (the same sensor was selected in each participant). As can be discerned, alpha/beta activity in this brain area strongly decreased (i.e., desynchronization) during the encoding phase, then shifted toward robust increases (i.e., synchronization) in a more narrow (alpha) band during the maintenance phase. Time periods with significant oscillatory activity (relative to baseline) were subjected to beamforming in 0.4 s non-overlapping time bins.

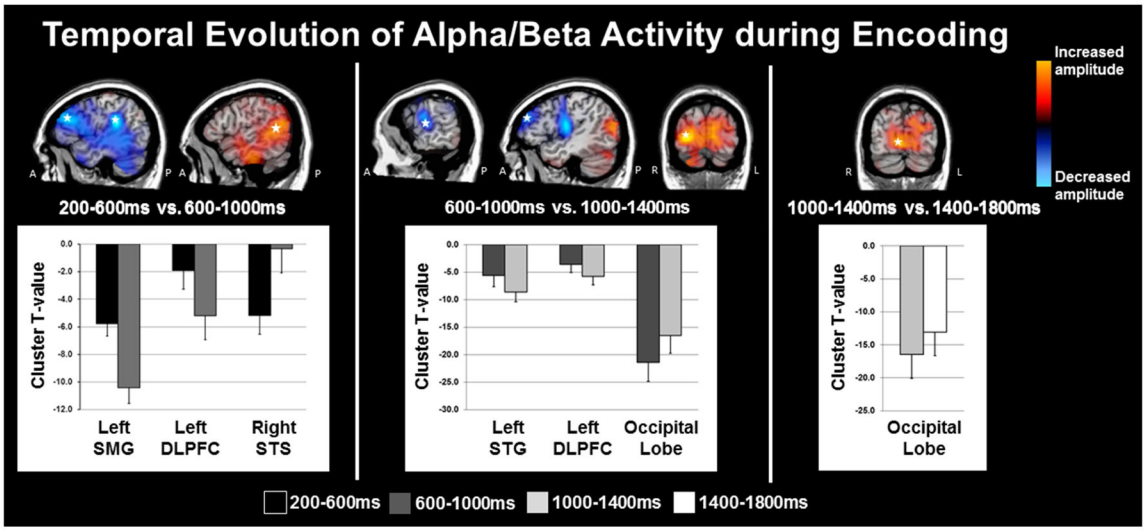

Figure 3.

Significant 9–16 Hz Oscillations during Encoding. Brain areas exhibiting significant changes in 9–16 Hz activity as a function of time are shown with red indicating increases in oscillatory power and blue showing decreases in power. For each cluster, the peak difference between time windows is denoted with a star on the top panel, and the t-values for the significant cluster (per time bin) are shown at the bottom. Note that the cluster t-values shown in the bar graphs were computed using a one-sample t-test on each time window, and are only meant to aid in interpreting the results of the paired-samples t-test; all p-values below were based on the paired-samples results. From Encoding 1 (0.2 – 0.6 s) to Encoding 2 (0.6–1.0 s), the amplitude of 9–16 Hz activity significantly decreased in the right superior temporal sulcus (STS; $p < .001$, corrected), while such activity significantly increased in the left DLPFC and supramarginal gyrus (SMG; both p's $< .001$, corrected). From Encoding 2 to Encoding 3 (1.0–1.4 s), the amplitude of activity in bilateral occipital cortices increased toward baseline levels ($p < .001$, corrected), while the significant decrease in 9–16 Hz activity continued in the left DLPFC and emerged in the superior temporal gyrus (STG: $p > 0.001$, corrected). Finally, from Encoding 3 to Encoding 4 (1.4–1.8 s) the significant increase in 9–16 Hz activity continued in the bilateral occipital cortices ($p < .001$, corrected).

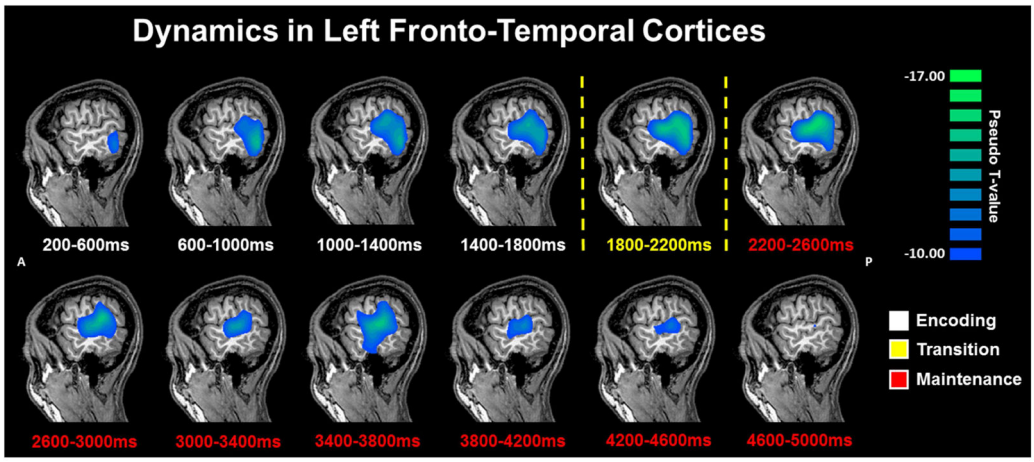

Figure 4.

Temporal Dynamics of Alpha/Beta oscillations in Left Fronto-Temporal Cortices. Group mean beamformer images (pseudo-t) of the encoding (blue) and maintenance (red) phases in each 0.4 s time bin starting 0.2 s after onset of the encoding grid. As can be discerned, there was a strong and sustained decrease in 9–16 Hz power throughout most of the encoding phase in the left middle and superior temporal gyri, and left supramarginal gyrus. Power decreased in these areas from Encoding 1 to Encoding 2, and from Encoding 2 to Encoding 3 (p's < .001, corrected). The response then stabilized in amplitude and was sustained throughout most of the maintenance period, until it clearly dissipated toward baseline near the end of the maintenance phase of the task, with significant changes in the last two time bins. It should be noted that there was also significant power decreases in the left DLPFC (see Results).

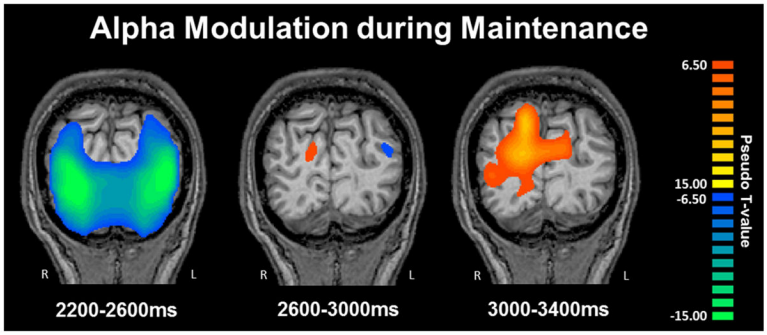

Figure 5.

Alpha Modulation during Maintenance. Group mean beamformer images (pseudo-t) of the maintenance phase showed a transition from a decrease (desynchronization) in the bilateral occipital cortices to a significant increase (synchronization) during the maintenance phase of the task, from 2.2 to 3.4 s (i.e., starting 0.2 s after the onset of the maintenance phase). Significant increases in activity within the cerebellum and occipital lobes occurred from Maintenance 1 to Maintenance 2 ($p > 0.001$, corrected), and from Maintenance 2 to Maintenance 3 ($p > 0.001$, corrected), where both responses turned into strong alpha synchronizations.